



Study of novel oxyfluoronitride bioglasses

A. Mabrouk ^a, A. Marrouche ^b, C. Follet ^c, A. Atbir ^b,
L. boukbir ^b, F. bentiss ^d, A. Bachar ^{b,e*}

^a CEMHTI CNRS UPR3079, 1D Av. de la recherche scientifique, 45071 Orléans Cedex 2, France

^b Laboratoire Génie des Procédés (LGP), Faculté des Sciences, Université Ibn Zohr, Agadir, Morocco

^c Laboratoire des Matériaux Céramiques et Procédés Associés, Université de Valenciennes et du Hainaut-Cambrésis, Valenciennes, France

^d Laboratoire de Catalyse et de Corrosion des Matériaux (LCCM), Faculté des Sciences, Université Chouaib Doukkali, B.P. 20, M-24000 El Jadida, Morocco

^e Campus Universitaire-Ait Melloul, Université Ibnou Zohr Agadir, Morocco

Received 29 Jun 2017,

Revised 07 Aug 2017,

Accepted 16 Aug 2017

Keywords

- ✓ Bioglass;
- ✓ Oxyfluoronitride glass;
- ✓ Physical properties;
- ✓ Mechanical properties;
- ✓ Bioactivity;
- ✓ Cytotoxicity

A. Bachar

a.bachar@uiz.ac.ma

Abstract

Bioglasses are used as bone substitutes and prosthetic coatings. Following implantation, they are predisposed to generate a series of physicochemical reactions at the glass-bone interface. Bioglasses with molar composition: $55\text{SiO}_2-8.5\text{CaO}-31.5\text{Na}_2\text{O}-5\text{CaF}_2$ have been synthesized and characterized. However, because of their poor strength, doping with nitrogen was performed on these glasses to increase their mechanical properties. The Young's elastic moduli, Vicker's microhardnesses, and the fracture toughnesses were measured and observed to increase linearly with nitrogen content in each of these systems. These results are consistent with the incorporation of nitrogen into the glass structure in three-fold coordination with silicon. Fluorine addition significantly decreases the thermal property values but the mechanical properties of these glasses remain unchanged with fluorine. The characterization of these N and F substituted bioglasses using ^{29}Si MAS NMR have shown that the increase in rigidity of the glass network can be explained by the formation of SiO_3N , SiO_2N_2 tetrahedra and Q^4 units with extra bridging anions at the expense of Q^3 units. The bioactivity of the glasses has been evaluated by soaking them in simulated body fluid (SBF) and showed that all oxyfluoronitrides glasses are bioactives. Cytotoxicity tests based on different concentrations of bioglass powders in a cell growth environment have been also showed that they are not cytotoxic

1. Introduction

Bioglass® [1] is known to bond to living bone in the body through formation of an apatite layer on its surface [1–5] and this has accelerated the search for new bioactive glasses and glass-ceramics with enhanced properties. However, the low strength and inherent brittleness of Bioglass® has restricted its use to nonload-bearing applications [1,2].

Bioglass® is known to bond to bone in the body through a sequence of surface reactions [6–8] with initial rapid release of soluble ionic species (Na^+ , Ca^{2+}) from the glass into the interfacial solution. A high surface area hydrated silica and polycrystalline hydroxyl carbonate apatite (HCA) bi-layer is formed on the glass surface within hours. The reaction layers enhance subsequent adsorption and desorption of growth factors and greatly decrease the length of time macrophages need to prepare the implant site for tissue repair. The HCA layer is similar to the mineral content of bone and the final stage of the process consists of crystallisation of the HCA which interacts with collagen fibrils so integrating with the host bone. Application of Bioglass® 45S5 particles to bone defects resulted in new bone growth during the first few weeks after surgery [9].

The low mechanical strength and inherent brittleness of these bioactive glasses restricted their use to non load-bearing applications [10] such as ossicles in the middle ear [11] and various maxillo-facial applications [12,13]. One way to increase strength of glasses is to introduce nitrogen into the silicate network [14,15]. It has been shown that when nitrogen replaces oxygen in silicate glasses, glass transition temperature, elastic modulus and hardness increase linearly with nitrogen content [16,17]. This is because N creates extra cross-linking of the

glass network and so may be viewed as a network forming anion taking in to account that the effects of nitrogen and modifiers on glass properties are independent [18] Mechanical properties have been shown to increase when nitrogen is incorporated into a Na-Ca-Si bioactive glass composition [19] Oxynitride glass-ceramics have also been shown to exhibit potential bioactivity [20]. The effect of fluorine addition on the structure of silicate or aluminosilicate glasses has been investigated by the other researchers [16]. The results show that fluorine can bond to silicon as Si-F, to Al as Al-F, and to Ca as Ca-F. Fluorine loss occurs under conditions where the Si-F bond is favoured. The bonding of fluorine to aluminum prevents the fluorine loss as SiF₄ from the glass melt and explains the reduction in the glass transition temperature [16].

The aim of the current work is to explore a new generation of bioglasses containing nitrogen and fluorine in the Si-Na-Ca-N-O-F system and to study the effects of nitrogen and fluorine on their structure and mechanical properties: hardness, elastic modulus and fracture toughness. Structural analysis of glasses was characterized using ²⁹Si and ¹⁹F MAS NMR spectroscopy. investigated. We decided also to study the effect of adding nitrogen on bioactivity and cytotoxicity of bioglasses. The bioactivity of the glasses has been evaluated by soaking them in simulated body fluid (SBF) [21]. The changes at the glass surface as a function of soaking time in the SBF was analyzed by X-ray diffraction (XRD). The cytotoxicity has also been studied with L132 epithelial cell line to assess the ability of the bioglasses for bone reconstruction. Cytotoxicity tests based on different concentrations of bioglass powders in a cell growth environment have been also evaluated.

Table 1: Atomic percentages of *of elements in prepared Na-Ca-Si-O-F base glasses (T – Theoretical; E – Experimental) obtained by EDS.*

At %	Si (±0.3)		Ca (±0.1)		Na (±0.2)		O (±0.4)		F (±0.1)		N (±0.1)	
	T	E	T	E	T	E	T	E	T	E	T	E
N0	18.87	21.87	4.63	3.87	21.61	22.87	51.46	48.97	3.43	2.42	0	0
N1	19.00	22.49	4.66	3.29	21.76	22.19	49.77	48.00	3.46	2.73	1.38	1.3
N2	19.13	22.77	4.70	3.24	21.92	21.90	48.29	46.75	3.48	3.04	2.48	2.3
N3	19.26	22.89	4.73	3.57	22.07	21.87	46.24	45.08	3.50	2.79	4.20	3.8
N4	19.40	23.00	4.76	3.58	22.32	21.58	44.45	44.56	3.51	2.78	5.65	4.5

2. Experimental and methods

2.1. Glass preparation

Oxyfluoronitride bioglasses of molar composition (55–3x)SiO₂–8.5CaO–31.5Na₂O–5CaF₂–xSi₃N₄ (x is the number of moles of Si₃N₄) were prepared by melting the glasses in two steps. Glasses were prepared from reagent grade SiO₂ (pure quartz, Merck), CaCO₃ (Chimie-Plus-Laboratoire, 99%), Na₂CO₃ (Merck, purity 99.9%), and CaF₂ (CarloErba, 98%) and Si₃N₄ (UBE, industries, minimum purity 98%). The weight of each reagent has been calculated taking into account their purity. The glasses were designed so that constant cation ratios could be maintained independently of nitrogen additions. Thus, the N:O ratio is the only composition variable which changes. The effects of cation ratio variations on glass structure and properties are eliminated. The compositions of the glasses are shown in Table 1. Base glasses were prepared by reacting and melting Na₂CO₃, CaF₂ and CaCO₃ with SiO₂ in a platinum crucible at 1350 °C in air. After this melting process, these oxide glasses were milled to a powder. The corresponding amount of Si₃N₄ to achieve the required composition was added to the glass powders taking into account the surface silica on the silicon nitride particles which were then milled in isopropanol in a ball mill with alumina media for 3 h and then the alcohol was evaporated. The powders were then pressed uniaxially under a pressure of 300 MPa to form pellets. The pellets were then placed in a BN lined graphite crucible and melted in a vertical tube furnace under flowing high purity N₂ at 1400 °C for 15 to 30 min. The glasses obtained were then annealed, at a temperature just below their glass transition temperature for 1 h, to stabilize the glass by eliminating stresses created by rapid cooling. Weights before and after melting were measured. The nitrogen concentrations retained in the glasses shown in Table 1, were determined by electron microprobe analysis using wavelength dispersive spectroscopy (WDS). The Si, Ca, Na and O relative contents were measured using scanning electron microscopy coupled with energy dispersive spectroscopy (SEM–EDS) with a Noran System Six-type. All glasses were also embedded into an epoxy resin and then polished with silicon carbide papers, graded from 80 to 1200. This provides a flat surface and easily analyzed by EDS, the analyzed area being about 1 μm³.

2.2. Characterisation of Glasses

In order to determine if the glasses were completely amorphous, samples were analysed using X-ray diffraction (XRD) (PanAlytical X-ray diffractometer, The Netherlands) with monochromated CuKα (λ=1.54056 Å)

radiation over a range of $2\theta = 20^\circ\text{--}80^\circ$ with a speed of $2.4^\circ/\text{min}$. Data was analysed using X'pert Quantify software.

The glass samples were embedded in epoxy resin and polished using SiC papers down to $0.25\ \mu\text{m}$ to provide a completely flat surface. Nitrogen analysis was carried out using wavelength dispersive spectroscopy (WDS) and a Cameca SX100 electron probe microanalyser (EPMA) at 15 kV and 200 nA. A PC2 (Ni/C) crystal was used to detect the $K\alpha$ X-rays. BN was used as a standard. 10 measurements were performed on each glass to assess nitrogen homogeneity and to determine the average nitrogen content. The background noise used for the calculation of the N $K\alpha$ peak height was measured on a glass without N. The relative Si, Ca, Na, O and F contents were measured on polished samples using scanning electron microscopy coupled with energy dispersive spectroscopy (SEM–EDS) (Noran System Six-type), the analyzed area being about $1\ \mu\text{m}^3$. The embedded glass samples were examined by Scanning Electron Microscopy (SEM) to analyse homogeneity and the presence of bubbles. Glasses without N, containing F, were free of bubbles but those without F contained some fine residual bubbles from loss of CO_2 during melting. F reduces melting temperatures and viscosities thus allowing easier gas evolution during melting. Glasses containing N always contained evidence of bubbles, both from CO_2 loss and from some loss of N, leaving macroporosity in the glasses. This has implications for further characterization of mechanical properties.

The density was measured using a Helium pycnometer. Glasses were crushed before density measurements so that any internal porosity (i.e. bubbles) did not affect the results. Differential thermal analysis (DTA) was carried out (Setaram Setsys 16/18 simultaneous

TG/DTA analyzer) in order to determine the glass transition temperature, T_g . Samples of 50 mg were heated at $10\ ^\circ\text{C}/\text{min}$ up to $1200\ ^\circ\text{C}$ in alumina crucibles in a flowing nitrogen atmosphere. Al_2O_3 was used as the reference material. T_g is taken as the inflexion point of the endothermic drift on the DTA curve.

The measurement of elastic properties by ultrasonic methods is based on the propagation velocities of ultrasonic waves inside the glasses. At room temperature, the elastic moduli (Young's E , Shear, G) were calculated from the measurement of the longitudinal, v_l and transverse, v_t , ultrasonic wave velocities with a better than $10^{-3}\ \text{m s}^{-2}$ accuracy by means of 10 MHz piezoelectric transducers.

The elastic moduli and Poisson's ratio, ν , are derived from the following relationships:

$$E = \rho \frac{v_l^2(4v_t^2 - 3v_l^2)}{(v_t^2 - v_l^2)} \quad (1)$$

$$G = \rho v_t^2 \quad (2)$$

$$\nu = \left(\frac{E}{2G}\right) - 1 \quad (3)$$

where ρ is the density of the material.

The accuracy of the measurement depends mainly upon the accuracy of the density measurement and the accuracy is then $\Delta E/E \approx 1\text{--}2\%$

Determination of Young's modulus, micro hardness and Vickers indentation fracture toughness measurements in the present work are as outlined by Bachar et al. [22].

2.3. Structural Analysis by ^{29}Si NMR

^{29}Si MAS NMR spectra were recorded at a Larmor frequency of 79.5 MHz using a Bruker Avance 400 MHz (9.4 T) spectrometer. The spectra were obtained with 96 scans with a pulse length of $1.7\ \mu\text{s}$ ($\pi/6$) and a relaxation delay of 300 s. The samples were spun at the magic angle of 54.7° and at spin rates of 5 kHz in 7 mm outer diameter zirconia rotors, with TMS (tetramethylsilane) used as reference. Spectral deconvolution was performed with Dmfit software [19].

2.4. Assessment of Bioactivity in Simulated Body Fluid (SBF)

Glass cylinders of dimensions 15 mm in diameter and 3 mm in height were polished with (2400 grit) silicon carbide coated paper. The polished glass pieces were ultrasonically cleaned in an isopropanol anhydrous bath. In vitro bioactivity tests were carried out on the dried glass plates by soaking them in simulated body fluid (SBF). SBF with ion concentration almost equal to that of human blood plasma was prepared by a procedure established by Kokubo et al. [24]. Accordingly, reagent grade NaCl, NaHCO_3 , KCl, $\text{K}_2\text{HPO}_4 \cdot 3\text{H}_2\text{O}$, $\text{MgCl}_2 \cdot 6\text{H}_2\text{O}$, CaCl_2 and Na_2SO_4 were dissolved in ion exchanged water and the resulting solution was buffered at a pH of 7.42 with 50 mM (tris-hydroxymethyl)-aminomethane and 45 mM hydrochloric acid. The temperature of the solution was maintained at $37\ ^\circ\text{C}$ throughout the experiment to simulate a human physiological environment. Glasses immersed in SBF were taken out after 15 days, gently rinsed in ion

exchanged water and stored in a vacuum desiccator. Structural changes on the surface of the samples treated in SBF were analyzed using grazing incidence XRD and SEM coupled with EDS spectroscopy.

2.5. Cytotoxicity

Cytotoxicity tests consist of viability tests which evaluate the relative plating efficiency (RPE) and subsequently the 50% lethal concentration LC50 (or RPE 50) by means of the colony-forming assay with epithelial cell line (L132 cells) [25]. According to the International and European Standards (ISO10993-5/EN30993-5), the L132 epithelial cell line is selected for its good reproducibility and cloning efficiency (about 37%) [26]. In minimum essential medium (MEM) supplemented with 10% foetal calf serum (FCS), the L132 cells are continuously exposed to gradually increasing concentrations (0, 25, 50, 100, 200, 400 mg L⁻¹) of bioglass powder (20 µm diameter granules) without renewal of the growth environment during the experiments. The positive control is pure nickel powder; the average particle size is 4-6 µm. After a 9-day culture period, the environment is removed and the colonies are stained with violet crystal. The number of colonies is then counted under a binocular microscope. At least six repeated experiments are performed, in triplicate for each concentration group. Results are expressed as mean values ± SD with respect to the control (an environment without glass powder, 100%). Nickel powder is also tested as a positive control for comparison.

3. Results and Discussion

3.1. Na₂O-CaO- CaF₂-SiO₂-Si₃N₄ Glass Synthesis and Characterisation

Homogeneous oxyfluoronitride glasses were successfully prepared and all synthesised materials were confirmed as amorphous by XRD (Figure 1). The Nx glasses were opaque and gray or black in colour. The most important reason for blackening of these types of glasses is known to be due to free silicon which come from the decomposition of Si₃N₄ or SiO₂ and this reacts with Fe from the impurities to promote FeSi₂ formation during cooling which changes the colour and transparency of glass [20]. Nx glasses (containing both F and N) contained smaller amounts of finer bubbles as a result of the lower viscosity of these melts, even at the lower melting temperature.

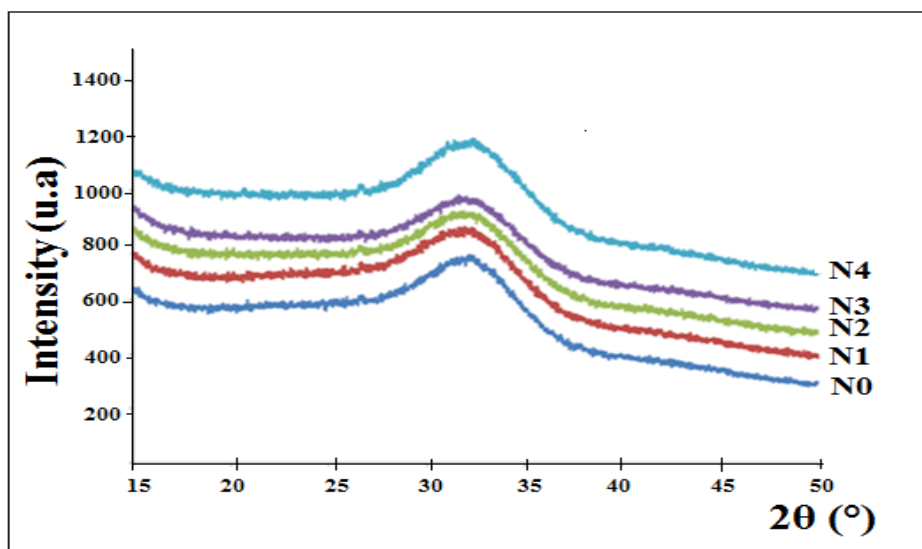


Figure 1: X-ray diffractograms of the Nx glasses

3.2. Thermal properties and density of Ca-Na-Si-O-N-F glasses.

The effect of nitrogen on the density of the Si-Ca-Na-O-F glasses is shown in Table 2. The variation in density observed with increasing nitrogen is quite significant and increases from 2.58 g/cm³ for N0 to 2.63 g/cm³ for N4 glass composition. Given that the only compositional variable which changes is N:O ratio, and that tri-coordinated N substitutes for di-coordinated O, then it is clear that for each % increase in nitrogen content the same number of extra cross-links are introduced into the glass network [16]. This will have the effect of contracting the network and therefore reducing molar volume and this is confirmed by the increase in density with increasing nitrogen content.

Table 2 shows that there is a significant increase in T_g and T_c with increasing nitrogen content. The glass transition temperatures for GFNx range from 473 °C to 537 °C as x increases from 0 to 4.5 atomic percentages.

Table 2: Thermal properties and density of the bioglasses Nx

Bioglass	T _g (°C)	T _c (°C)	Density (g/cm ³)
N0	473	592	2.586
N1	490	609	2.605
N2	508	628	2.614
N3	526	646	2.627
N4	537	715	2.631

Both ions F and N affect the motion of structural units in the glass. Cross-linked nitrogen keep the units more rigidly fixed and therefore there is an increase in the thermal energy required for segmental mobility and thus an increase in T_g [27].

3.2. Mechanical properties of Si-Na-Ca-O-N-F.

Vickers hardness HV, elastic modulus E and VIF toughness K_c measured by indentation methods and corresponding standard deviations are in table 3. HV and E were calculated for P=500 g. Elastic modulus measured by an ultrasonic method are also indicated in the same Table 3.

Table 3: Hardness (HV), elastic modulus (E) and VIF toughness (K_c) results measured by indentation methods for GFNx glasses

Bioglass	N0	N1	N2	N3	N4
N wt. %	0	0.86	1.71	2.54	3.01
HV (GPa)	5.34 ± 0.11	5.5 ± 0.17	5.9 ± 0.15	6.45 ± 0.12	6.65 ± 0.12
E(GPa) indentation method	63.6 ± 2.8	71 ± 3.3	80.6 ± 2.5	89 ± 4.5	92.5 ± 6.2
E(GPa) ultrasonic method	63 ± 1	70 ± 2	79 ± 1	87 ± 2	91 ± 2
Meyer's index n	1.92	1.94	2.06	2.01	1.98
ln(c)-ln(P) slope	0.671	0.682	0.679	0.681	0.679
K _c (MPa.m ^{1/2})	1.03 ± 0.03	1.09 ± 0.04	1.21 ± 0.04	1.46 ± 0.08	1.64 ± 0.08

Microhardness increases with nitrogen content from 5.3±0.2 GPa for 0 at.%N to 6.7±0.1 GPa (24% increase) at 4.5 at.% N for the GFNx glass series. Microhardness can be modelled by the following empirical relationships:

$$HV \text{ (GPa)} = 5.3 + 0.30 [N] \quad (4)$$

where [N] is N content in at.%.

the elastic modulus increases with increasing nitrogen content, from 64±3 GPa for 0 at.% N to 93±6 GPa (45% increase) at 4.5 at.% N for the Nx series. The variation appears to be linear, and can be modelled by the following empirical relationships:

$$E \text{ (GPa)} = 64 + 4.30[N] \quad (5)$$

where [N] is N content in at.%.

The substitution of nitrogen for oxygen in the glass results in an increase in K_{ifr} from 1.0 MPa.m^{1/2} at 0 at.% N to 1.6 MPa.m^{1/2} at 4.5 at.% N for Nx series (60% increase). , the experimental results can be modelled by a power law, in the range 0 to 4.5 at.% N, as follows:

$$K_{ifr} = K_{ifr0} + m [N]^n \quad (6)$$

where K_{ifr0}, m are constants, [N] is N content in at.% and n is the exponent. K_{ifr0} is considered to be the VIF resistance of the base glass with 0 at.% N. Thus, as shown in table 3, the change in K_{ifr} with nitrogen is given by the following empirical relationships:

$$K_{ifr} \text{ (MPa.m}^{1/2}\text{)} = 1.0 + 0.01 [N] + 0.025 [N]^2 \quad (7)$$

For the oxynitride bioglasses prepared in this work, it was shown that the Vickers hardness, Young's modulus and VIF resistance increased with increasing nitrogen content. This indicates that the incorporation of nitrogen stiffens the network structure of glass. This increase in rigidity of the glass network can be explained by the

extra cross-linking provided by the trivalent N³⁻ ion in place of the divalent O²⁻ ion with formation of SiO₃N and SiO₂N₂ tetrahedra, each of which will have extra bridging anions compared with SiO₄.

3.2. ²⁹Si MAS NMR

Figure 2 shows the ²⁹Si MAS NMR spectra of N0, N2 and N4 glasses. In the spectrum of the N0 glass, the main contributions in the signal are located around -78.1 and -85.3 ppm, attributed respectively to Q² (37%) and Q³ (63%) units [28].

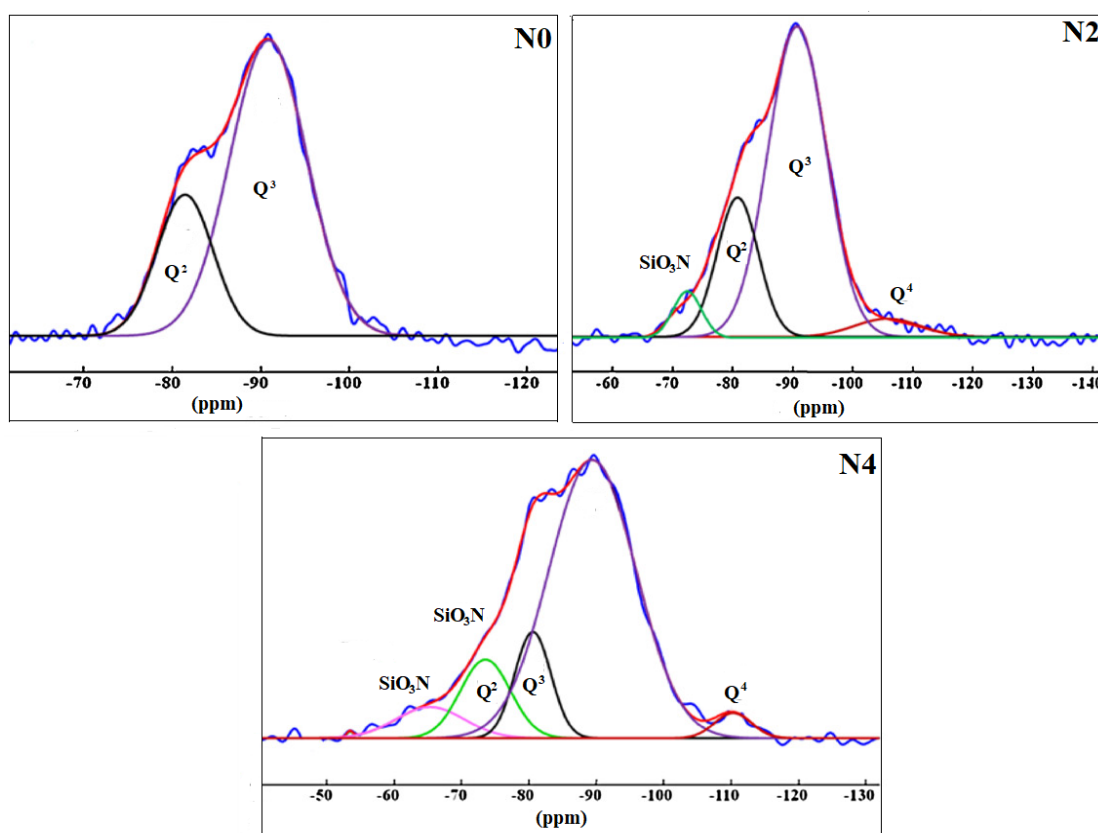


Figure 2: Deconvolution of ²⁹Si NMR MAS spectra of Nx glasses

Introduction of nitrogen into the anionic network brings a wider variety of silicon environments. Two new bands around -70 and -59 ppm appear, attributed to [SiO₃N] and [SiO₂N₂] units, respectively [29]. When nitrogen is initially introduced, SiO₃N tetrahedra are formed with a reduction in Q³ units. Further addition of nitrogen results in more SiO₃N tetrahedra, fewer Q³ units and the appearance of small amounts of Q⁴ units and SiO₂N₂ tetrahedra. Further increase of N leads to further small increases in Q⁴ units and SiO₂N₂ tetrahedra, even at the expense of SiO₃N tetrahedra as well as Q³ units. The quantity of Q² units decreases only slightly as nitrogen content increases

3.3. Bioactivity In vitro tests

The XRD patterns of the glasses before immersion in SBF solution are characterized by an amorphous halo confirming that all the glasses were amorphous. The XRD patterns obtained from all Nx samples after immersion in SBF for 15 days are presented in Figure 3. The natural hydroxyapatite pattern is used as a reference (JCPDS pattern no. 90432) and also for comparison. It shows that on all the glass samples, a hydroxyapatite layer is formed, confirmed by the three strongest XRD peaks appeared at 2θ of 26.30, 32.27 and 53.15° that correspond, respectively, to the (002), (112) and (004) planes. However, the intensities of the major peaks (002), (112) and (004) decrease with nitrogen content showing that the crystallinity of this layer consistently decreases with its content, suggesting that nitrogen may inhibit bioactivity. Therefore, the crystallization of the apatite layer is slowed down when the doping elements were added.

The SEM micrographs of the bioactive glasses immersed for 15 days in the SBF are presented in the Figure 4.

On pure N0 and doped glasses N4, an apatite layer is formed. Morphologies of apatite crystals, their sizes and their reliefs are different according to the rate of nitrogen and their content.

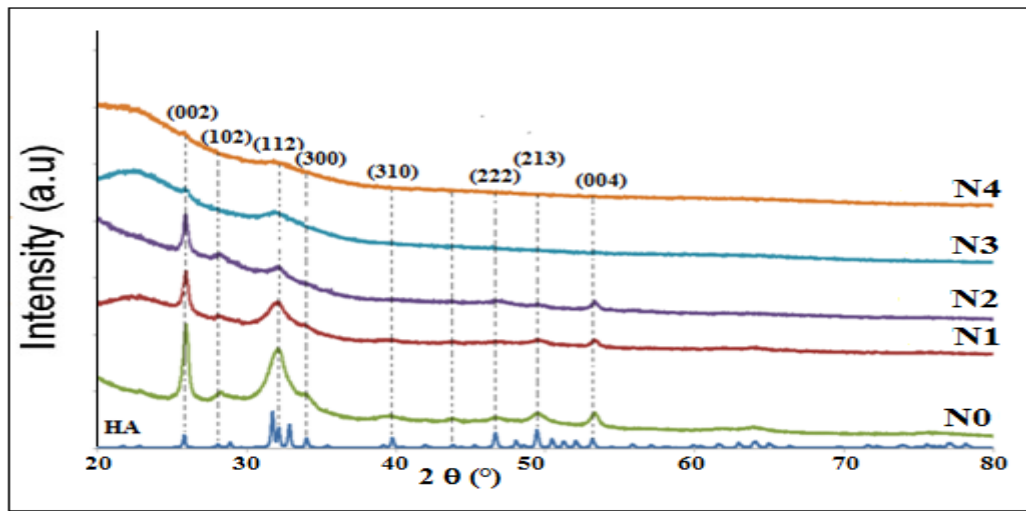


Figure 3: X-ray diffraction patterns of Nx bioactive glasses after soaking in SBF solution for 15 days

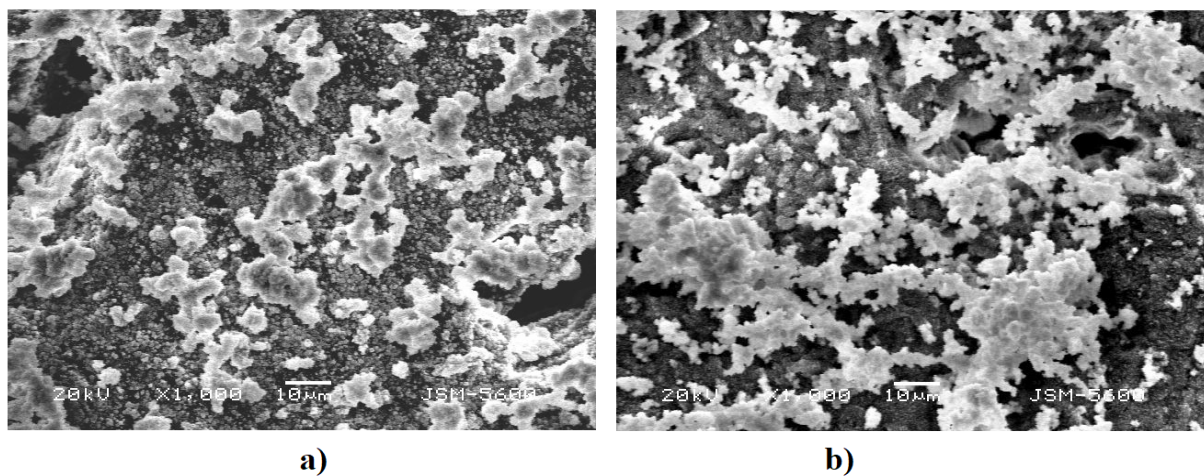


Figure 4: SEM micrograph of the: a) N0 and b) N4 glasses surface after soaking in SBF

Indeed, for N0 (Figure 4a), the apatite layer is homogeneous. The apatite layer of N4 (Figure 4b) has almost the same morphology and the same relief but the size of crystals is different and the apatite layer is more heterogeneous. These micrographs confirm the XRD results showing the slowdown of the hydroxyapatite crystals growth. Moreover, a better crystallization of hydroxyapatite is observed with a low rate of nitrogen. The mechanism of apatite deposition on the surface of $\text{Na}_2\text{O-CaO-SiO}_2$ glasses in the simulated body fluid has been reported by Ohtsuki et al. [30]. When these materials are exposed to SBF for a period of time, Ca and Si ions are released and silanol groups (Si-OH) form on the surface of the material.

3.4. Cytotoxicity

Figure 5 shows the results of viability tests, performed on samples of Nx and nickel powder as a function of powder concentration. The viability percentage is determined by the ratio between the number of surviving L132 cells in the medium exposed to the powder sample and the number of surviving cells in a control medium. LC 50 corresponds to the death of 50% of the cells. The number of introduced cells is the same in all the samples and the control. It is necessary to compare with the control because the survival ratio is never really 100%. Indeed, the cells are stressed during the subculture which leads to the death of a small fraction.

A compound will be considered cytotoxic if its addition into the culture medium increases the cell death as the compound concentration increases. In the present case, bioglasses Nx do not show this behavior. With a concentration of 400 mg L^{-1} the average survival of L132 cells is 100% for G1Nx. Thus, neither of the glasses are cytotoxic. It is interesting to note that both bioglasses show a higher survival ratio than 100% at low concentrations (112% for N0 and 105% for N4 with 25 ml L^{-1}). This result shows that the bioglasses improve growth conditions for cells which might reduce the stress on the L132 cells.

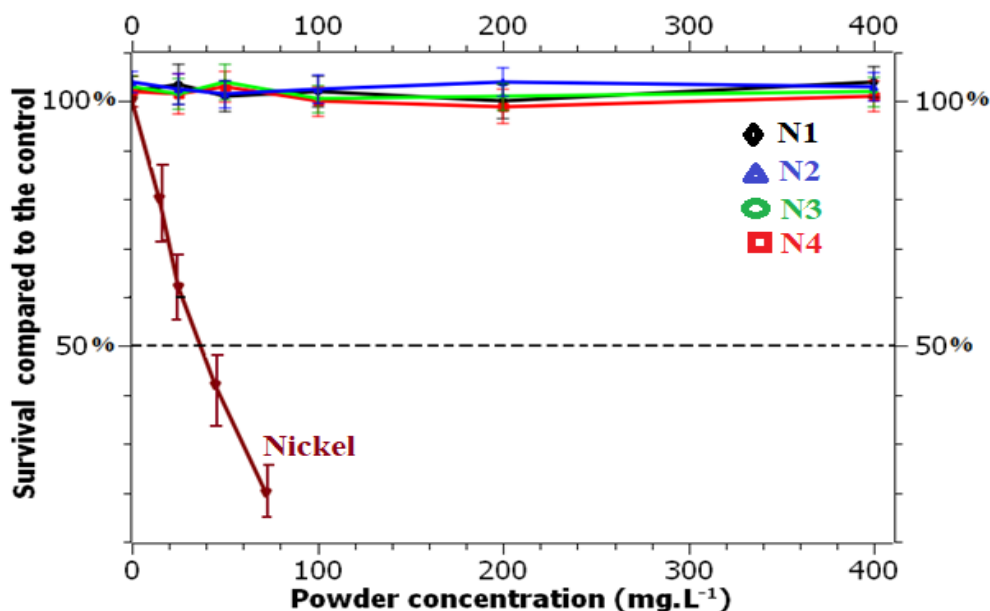


Figure 5: L132 viability tests on Nx and nickel

Conclusions

Oxyfluoronitride bioglasses of molar composition $(55-3x)\text{SiO}_2-8.5\text{CaO}-31.5\text{Na}_2\text{O}-5\text{CaF}_2-x\text{Si}_3\text{N}_4$ (x is the number of moles of Si_3N_4) have been synthesized and characterized. The following conclusions can be made regarding the effect of composition on properties and structure:

- 1) The density increases with nitrogen content which means that incorporation of N results in a higher compactness of the glass network and therefore a lower molar volume. Glass transition temperature, hardness and elastic modulus all increased linearly with nitrogen content which indicates that the incorporation of nitrogen stiffens the glass network because N is in three-fold coordination with silicon which results in extra cross-linking.
- 2) The characterization of these oxynitride bioglasses using ^{29}Si MAS NMR and infrared spectroscopy have shown that this increase in rigidity of the glass network can be explained by the formation of SiO_3N , SiO_2N_2 tetrahedra and Q^4 units with extra bridging anions at the expense of Q^3 units
- 3) Following immersion of the glasses in SBF for 15 days, a homogeneous layer of hydroxyapatite crystals with diameters of 200–300 nm was formed on the surfaces of both series of glasses. The crystallinity of this layer decreases with N content suggesting that N may inhibit bioactivity.
- 4) All bioglasses N_x show a higher survival ratio than 100% at low concentrations, the cytotoxicity tests show that they are not cytotoxic.

References

1. L.L. Hench, *J. Am. Ceram. Soc.* 74 (1991) 1487–510.
2. L.L. Hench., R.J. Splinter, W.C. Allen, T. K. Greenlee, *J. Biomed. Mater. Res. Symp.* 2 (1971) 117–41.
3. L.L. Hench, J.K. West, *Life Chem. Rep.* 13(1996) 187–241.
4. S. Fujibayashi, M. Neo, H. Kim, T. Kokubo, T. Nakamura, *Biomaterials* 24 (2003) 1349–56.
5. R. Hill, *J. Mater. Sci. Letts.* 15 (1996) 1122 5.
6. S. Chajri, S. Bouhazma, S. Herradi, H. Barkai, S. Elabed, S. Ibsouda Koraichi, B. El Bali, M. Lachkar, *J. Mater. Environ. Sci.* 6 (Y) (2015) 1882-1897
7. J.J. Hren, P.F. Johnson, S.R. Bates, L.L. Hench, *Proc Electron Microsc Soc Amer 34th Ann Mtg.* Claitor's Publishing, (1976) 290-291.
8. C.Y. Kim, A.E. Clark, L.L. Hench, *J Non-Cryst Sol.* 13(1989) 195-202.
9. H. Oonishi, L.L. Hench, J. Wilson, F. Sugihara, E. Tsuji, *J. Biomed. Mater. Res.* 51 (2000) 37–46.
10. K.R Rust, G.T. Singleton, J. Wilson, P.J. Antonelli, *Am J Otolaryngol.* 17 (1996) 371–374.
11. J.R. Jones., *Acta Biomater* 9 (2013) 4457–4486.
12. H.R. Stanley, M.B. Hall, A.E. Clark, C.J. King, L.L. Hench, *Int J Oral Maxill. Imp.* (1997) 95–105.
13. I.D. Thompson, *New materials and technologies for healthcare. Singapore:World (2011)* 77–96.
14. S. Hampshire, R.A.L. Drew, K.H. Jack, *PhysChem Glasses* 26 (1985) 182-186.

15. S. Hampshire, M.J. Pomeroy, *Int J ApplCeram Tech* (2008)155-163.
16. M.J. Pomeroy, S. Hampshire, *J Ceram Soc Jap.* 116 (2008)755-761.
17. P. Becher, S. Hampshire, M.J. Pomeroy, M. Hoffmann, M. Lance, Satet R., *Int J Appl Glass Sci.* 2 (2011) 63-83.
18. M.J. Pomeroy, E. Nestor, R. Ramesh, S. Hampshire, *J. Am. Ceram Soc.* 88 (2005) 875-881.
19. A. Bachar, C. Mercier, A. Tricoteaux, A. Leriche, C. Follet, M. Saadi, S. Hampshire, *J. Non-Cryst.Sol.* 358 (2012) 693-701.
20. A.R. Hanifi, C. Crowley, Pomeroy M.J., Hampshire S., *J Mater Sci.* 49 (13) (2014) 4590-4594.
21. R.L. Siqueira, O. Peitl, E.D. Zanotto, *Materials Science and Engineering:C*, 31 (2011) 983-991.
22. A. Bachar, C. Mercier, A. Tricoteaux, S. Hampshire, A. Leriche, C. Follet, *Jour. Mech. Beh. Biom. Mat.* 23 (2013) 133-148.
23. D. Massiot, F. Fayon, M. Capron, I. King, S. Le Calvé, B. Alonso, J.O. Durand, B. Bujoli, Z. Gan, G. Hoatson, *Magn Reson in Chem.* 40 (2002) 70-76.
24. T. Kokubo, *Journal of Non-Crystalline Solids.* 120 (1990) 138-151.
25. M.E. Frazier, T.K. Andrews, Raven Press, New York. (1979) 71-81.
26. J.C. Hornez, A. Lefèvre, D. Joly, H.F. Hildebrand, *Biomolecular Engineering.* 19 (2002) 103-117.
27. A. Bachar, C. Mercier, C. Follet, N. Bost, F. Bentiss, S. Hampshire, *J. Mater. Environ. Sci* 7 (2016) 347-355.
28. C. Mercier, C. Follet-Houttemane, A. Pardini, B. Revel, *J Non-Cryst Sol.* 357 (2011) 3901.
29. R.S. Aujila, G. Leng-Ward, M.H. Lewis, E.F.W. Seymour, G.A. Styles, *Philos Mag B* 6 (1986) 54-51.
30. C. Ohtsuki, T. Kokubo, T. Yamamuro, *Journal of Non-Crystalline Solids.* 143 (1992) 84-92.

(2018) ; <http://www.jmaterenvirosci.com>